Nanocast mesoporous $MgAl_2O_4$ spinel monoliths as support for highly active gold CO oxidation catalyst

Wen-Cui Li, Massimiliano Comotti, An-Hui Lu and Ferdi Schüth*

Received (in Cambridge, UK) 24th January 2006, Accepted 6th March 2006
First published as an Advance Article on the web 17th March 2006
DOI: 10.1039/b601109h

Mesoporous $MgAl_2O_4$ spinel monolith was synthesized by the nanocasting pathway; high activity in CO oxidation was observed over gold catalysts based on such monoliths as support.

$MgAl_2O_4$ spinel is a material widely used as a refractory due to its high melting temperature (2135 °C).[1] The same property and its hydrothermal stability make it also promising for applications as a catalyst or catalyst support in environmental catalysis, petroleum processing, and fine chemicals production.[2] However, for such applications, in contrast to uses as a refractory material, high surface area and small particle sizes are desirable. Over the last few years, nanosized spinels have been prepared by sol-gel processing,[3] coprecipitation,[4] solid state reactions,[5] controlled conversion of zeolites,[6] and other routes. In these cases, high temperatures of up to 1600 °C are often required to produce the spinel phase, and control of the pore structure of the spinel is not easy. Nanocasting as a versatile strategy is attracting considerable attention due to its simplicity.[7] In this pathway, the voids of a hard template, normally porous silica or carbon, are impregnated with precursors of the desired composition. The subsequent solidification and removal of the template may lead to a negative replica. Valdés-Solís proposed the use of a silica xerogel as a template to prepare nanosized spinels and perovskites.[8] The resulting spinels obtained after leaching the silica with NaOH are characterized by surface areas close to 100 $m^2 g^{-1}$. Alternatively, porous carbon materials could be used as hard templates, since the carbon template can easily be removed by combustion.[9] Moreover, the pore structure of carbons can be controlled to some extent by varying the synthetic conditions.[10] This provides an opportunity for the synthesis of porous oxides or spinels with controllable size and desired chemical composition. Several nanostructured materials including MgO,[11] Al_2O_3,[12] and zeolites[13] with tunable textural parameters have been prepared by nanocasting with porous carbon as template in our laboratory. Here we describe the extension of this approach to a spinel type monolithic ternary oxide, $MgAl_2O_4$. Due to its favorable properties, the application of the resultant $MgAl_2O_4$ as a gold catalyst support has been explored.

Gold catalysts are highly active in many reactions including CO oxidation, water-gas shift reaction, propylene epoxidation *etc.* Gold catalysts obtained by deposition of nanometer sized particles on metal oxides such as TiO_2,[14] Al_2O_3,[15] MgO,[16] or La_2O_3[17] show high catalytic activity in CO oxidation even below room temperature. However, the most attractive application is preferential CO oxidation in reformate streams as feed for PEM fuel cells, which always takes place in an atmosphere containing H_2, CO_2, and water. For such gas compositions, the high stability of $MgAl_2O_4$ spinel seems to be attractive, which is the reason for the exploration of its suitability as a support in CO oxidation.

The template carbon aerogel monolith for the synthesis of $MgAl_2O_4$ was prepared through the resorcinol–formaldehyde polymerization route.[10] A mixed solution of magnesium nitrate and aluminium nitrate with an appropriate ratio was prepared in deionized water. Prior to impregnation, the carbon aerogel was exposed to the gas phase over an ammonia solution in order to introduce hydrophilic nitrogen-containing groups on the surface and thus facilitate impregnation, and then immersed in the metal nitrate solution for up to 12 h to ensure satisfactory impregnation. The FTIR spectrum (not shown) confirms that the ammonia treated carbon aerogel possesses nitrogen-containing groups (new bands appeared at 3209 cm^{-1} and 1401 cm^{-1}), which enhance the achievable loading of the spinel precursor. The drying step was performed at the low temperature of 50 °C to prevent a possible decomposition of metal nitrate. The sample was then heat-treated to 850 °C under argon to form the $MgAl_2O_4$ spinel phase. Repetition of the impregnation and heat-treatment steps is advantageous, since it improves the mechanical stability of the spinel monolith. Finally, the white colored spinels were collected after the carbon template had been burnt out at 600 °C in air. Four carbon aerogels with different textural properties, in sequence denoted as CA-1 to CA-4, were selected as templates and the corresponding spinel products are named $MgAl_2O_4$-1 to $MgAl_2O_4$-4.

X-ray diffraction (XRD) patterns of the samples recorded with a Stoe STADI P diffractometer (transmission geometry) are shown in Fig. 1. All the samples only have reflections which can be assigned to the $MgAl_2O_4$ spinel phase (JCPDS-21-1152). No MgO or Al_2O_3 was detected for either of these samples. The XRD reflections of $MgAl_2O_4$-3 and $MgAl_2O_4$-4 are broader compared to those of $MgAl_2O_4$-1 and $MgAl_2O_4$-2, indicating a smaller crystallite size, which can be further confirmed by the crystallite size estimated from the Scherrer equation (Table 1).

Nitrogen adsorption measurements for the carbon templates and the spinels were performed at 77 K and the isotherms are plotted in Fig. 2. The calculated textural parameters of all the spinels and carbon templates are summarized in Table 1. As reported in Fig. 2 (left), the isotherms of both carbons have a clear hysteresis loop. However, it is located in the relative pressure range of 0.8–1.0 for CA-2 and 0.4–1.0 for CA-4, indicating a different mesopore size for these two carbons (CA-1 and CA-3 have an isotherm shape similar to CA-2 and CA-4, respectively, therefore

Max-Planck-Institut für Kohlenforschung, Mülheim an der Ruhr, 45470, Germany. E-mail: schueth@mpi-muelheim.mpg.de; Fax: 49 208 3062995; Tel: 49 208 3062373

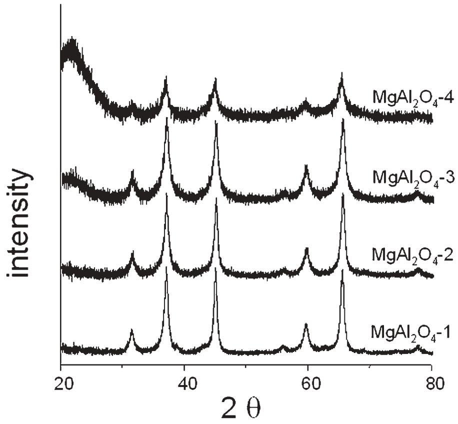

Fig. 1 XRD patterns of spinels synthesized using different carbon aerogels.

they are not shown here). The dominant pore sizes are around 18 nm for CA-2 and 6 nm for CA-4 (Fig. 2 left, insert). After removal of the carbon template, MgAl$_2$O$_4$-1 and MgAl$_2$O$_4$-2 maintain the monolithic shape of the parent carbon template. However, MgAl$_2$O$_4$-3 and MgAl$_2$O$_4$-4 are obtained in powder form. The difference can be explained if one considers the yield of the spinels. MgAl$_2$O$_4$-1 and MgAl$_2$O$_4$-2 are formed in more than 50% yield based on the weight of carbon templates. In contrast, only around 20% yield was achieved for spinels MgAl$_2$O$_4$-3 and MgAl$_2$O$_4$-4 generated from CA-3 and CA-4. Such a low loading with spinel is not sufficient for a fully connected, mechanically stable monolith after the combustion step, which consequently causes collapse of the pore structure. In Fig. 2 (right) it can be seen that MgAl$_2$O$_4$-2 has a similar isotherm shape to its template CA-2, *i.e.* an obvious hysteresis loop at relative pressure of 0.8–1.0. The dominant pore size is located at around 10–20 nm, a little smaller than that of the corresponding carbon template. Such a deviation is not surprising because the negative replica always reflects the particle size of the template rather than the pore size. As a result of the low yield, the hysteresis loop of MgAl$_2$O$_4$-4 becomes smaller and shifts to high relative pressure of 0.8–1.0, which is significantly different from that of the mother template CA-4. The inserted profile in Fig. 2 (right) shows a large and broad pore size distribution (PSD) for MgAl$_2$O$_4$-4. Obviously, a low yield of spinel results in collapse of the material, and spinel crystallites are agglomerated with each other to form a new interparticle mesopore system with large sizes and broad PSD. Comparing the textural parameters of the spinels listed in Table 1, MgAl$_2$O$_4$-3 and MgAl$_2$O$_4$-4 have very high surface area of around 200 m^2 g^{-1} and high pore volume close to 1 cm^3 g^{-1}. Such high surface area and, especially, such high pore volume have rarely been reported in the published literature. The high pore volume can be attributed to the contribution of the interparticle mesopore system generated from agglomeration of spinel crystallites. MgAl$_2$O$_4$-1 and MgAl$_2$O$_4$-2 have surface areas over 100 m^2 g^{-1} and pore volume below 0.3 cm^3 g^{-1} due to a high loading resulting in a condensed framework.

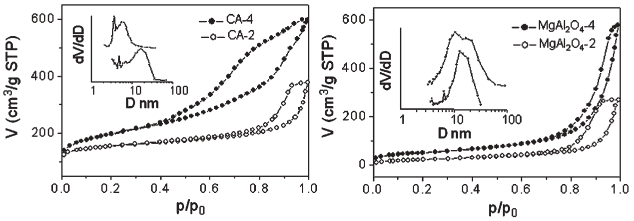

Fig. 2 Sorption isotherms and pore size distributions of carbon aerogel templates (left) and replicated MgAl$_2$O$_4$ spinels (right).

Representative spinel and carbon template samples were characterized by transmission electron microscopy (TEM), and the TEM images are shown in Fig. 3. As seen in Fig. 3 (top), spinel MgAl$_2$O$_4$-1 contains a three dimensional framework consisting of small particles with uniform size, which is quite similar to the structure of the mother template CA-1 (Fig. 3 bottom). At high resolution, the estimated particle size of the spinel is in the range 8–10 nm, which is in good agreement with the results obtained from XRD patterns (Table 1). Moreover, it is important to notice that the TEM pictures only show completely crystalline particles which can be inferred from the lattice fringes, and no amorphous phase is visible. The particle size of the carbon template is roughly

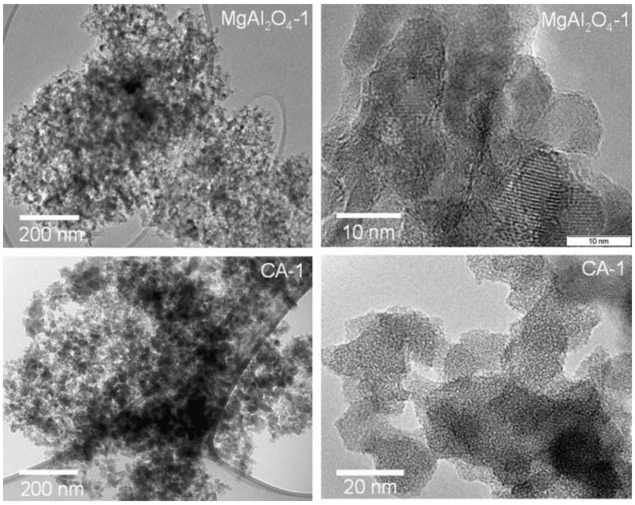

Fig. 3 TEM images of spinel MgAl$_2$O$_4$-1 (top) and the corresponding carbon template CA-1 (bottom).

Table 1 Texture parameters of carbon aerogel templates and the corresponding MgAl$_2$O$_4$ spinels[a]

Template					Spinel					
Sample	S_{BET}/m^2 g^{-1}	V_{mic}/cm^3 g^{-1}	V_{tot}/cm^3 g^{-1}	D/nm	Sample	Yield (%)	S_{BET}/m^2 g^{-1}	V_{mic}/cm^3 g^{-1}	V_{tot}/cm^3 g^{-1}	Particle size/nm
CA-1	626	0.18	0.76	22.4	MgAl$_2$O$_4$-1	60.1	110	—	0.24	11.2
CA-2	628	0.20	0.49	17.5	MgAl$_2$O$_4$-2	47.9	107	0.01	0.29	8.3
CA-3	600	0.11	0.80	6.6	MgAl$_2$O$_4$-3	14.1	201	0.01	1.13	5.8
CA-4	687	0.11	0.87	5.8	MgAl$_2$O$_4$-4	28.5	186	0.01	0.67	5.4

[a] S_{BET}: BET surface area; V_{mic}: micropore volume; V_{tot}: total pore volume; D: dominant pore diameter.

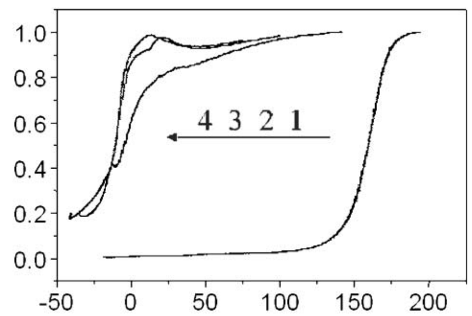

Fig. 4 Activity of $Au/MgAl_2O_4$ catalyst in CO oxidation. The four curves represent the results of four individual test cycles.

15–20 nm, and these particles are cross-linked with each other to form a pearl-like cluster structure, resulting in the formation of mesopores of 15–20 nm in diameter. In principle, as a negative replica, the particle size of the spinel should reflect the pore size of the mother template if the nanocasting step is performed perfectly. In our case, the particle size of the spinel is somewhat smaller than the pore size of carbon. However, this is understandable since only around 60% of the pore space of the carbon was filled with the spinel and thus particle sizes are expected to be smaller than the pore sizes.

Due to strong interest in using the $MgAl_2O_4$ spinel as a gold catalyst support, sample $MgAl_2O_4$-1 was selected to be loaded with gold nanoparticles by the colloidal deposition method.[18] The gold particle size as estimated by high-resolution TEM is around 1–4 nm, and mostly below 2 nm. The activities of the catalysts for CO oxidation were measured in a plug flow reactor using 50 mg of sieved catalyst (250–500 μm) in a gas mixture of 1% CO in air at a flow rate of 67 ml min^{-1}. Experiments were carried out under transient conditions: the reactor was cooled down to −40 °C prior to each experiment under a flow of nitrogen, which was then replaced by the gas mixture, after the base temperature had been reached. Subsequently, the temperature was ramped with a rate of 2 °C min^{-1} to the final temperature. Temperature for 50% conversion ($T_{50\%}$) was used as an index to evaluate the activity of the catalysts. This had previously been shown to give reliable and comparable catalytic data.[18]

The prepared $Au/MgAl_2O_4$ was tested in CO oxidation in four subsequent runs; the results are reported in Fig. 4. Surprisingly and unexpectedly, this catalyst was extremely active in CO oxidation, showing a mean temperature of half conversion ($T_{50\%}$) of −9 °C except for the first run, which is required for the "activation" of the catalyst. This is due to the inhibitory effect of the protecting agent which needs to be removed first, and is typical of the colloidal preparation method used here.[18] The high activity is quite similar to that of Au/TiO_2, which is well known to be one of the most active gold catalysts in CO oxidation.[14] Up to now, only one patent by Grunwaldt and Teunissen has reported the use of $Au/MgAl_2O_4$ catalyst, for the preferential oxidation of CO in a hydrogen containing process stream.[19] They found that $Au/MgAl_2O_4$ is not only a suitable catalyst for CO oxidation in inert gases, but also for preferential CO oxidation in gas mixtures containing CO, H_2, CO_2, and/or water. They also reported that Au/Al_2O_3 and $Au/Mg(OH)_2$ catalysts prepared by the same method were less active, and in particular for $Au/Mg(OH)_2$ deactivation occurred in presence of CO_2. Although the different operation conditions in the two cases do not allow a comparison between our results and the ones reported in the patent, $MgAl_2O_4$ spinel is evidently a highly active support for gold catalysts, and we are now also exploring its activity in other reactions.

Due to the difficulties often encountered in reproducing both the synthesis of gold catalysts as well as catalytic tests, we checked the reproducibility of our $Au/MgAl_2O_4$ catalyst. Satisfactorily, samples from different batches show nearly identical activity, with $T_{50\%}$ deviating less than ±10 °C.

In summary, we have reported the synthesis of $MgAl_2O_4$ monolith by a nanocasting pathway using monolithic carbon aerogel as the template. The prepared spinel is mesoporous, with a high surface area of up to 200 $m^2\ g^{-1}$ and particle sizes in the range 5–10 nm. Generalization of the method is probably possible to produce other high surface area spinels, perhaps even other ternary or multinary oxide phases, which are not easily achieved by conventional methods. Gold supported on the $MgAl_2O_4$ spinel by colloid deposition shows a very high activity in CO oxidation with a temperature of 50% conversion of around −10 °C.

Notes and references

1 J. Mori, W. Watenabe, M. Yoshimura, Y. Oguchi and T. Kawakami, *Am. Ceram. Soc. Bull.*, 1990, **69**, 1172.
2 J. Salmones, J. A. Galicia, J. A. Wang, M. A. Valenzuela and G. Aguilar-Rios, *J. Mater. Sci. Lett.*, 2000, **19**, 1033; O. R. Evans, A. T. Bell and T. D. Tilley, *J. Catal.*, 2004, **226**, 292.
3 J. Guo, H. Lou, H. Zhao, X. Wang and X. Zheng, *Mater. Lett.*, 2004, **58**, 1920.
4 J. Guo, H. Lou, H. Zhao, D. Chai and X. Zheng, *Appl. Catal., A*, 2004, **273**, 75.
5 I. Ganesh, B. Srinivas, R. Johnson, B. P. Saha and Y. R. Mahajan, *J. Eur. Ceram. Soc.*, 2004, **24**, 201; L. Schreyeck, A. Wlosik and H. Fuzellier, *J. Mater. Chem.*, 2001, **11**, 483.
6 W. Schmidt and C. Weidenhaler, *Chem. Mater.*, 2001, **13**, 607; W. Schmidt and C. Weidenhaler, *Microporous Mesoporous Mater.*, 2001, **48**, 89.
7 H. Yang and D. Zhao, *J. Mater. Chem.*, 2005, **15**, 1217; F. Schüth, *Angew. Chem., Int. Ed.*, 2003, **42**, 3604.
8 T. Valdés-Solís, G. Marbán and A. B. Fuertes, *Chem. Mater.*, 2005, **17**, 1919.
9 A.-H. Lu, W. Schmidt, A. Taguchi, B. Spliethoff, B. Tesche and F. Schüth, *Angew. Chem., Int. Ed.*, 2002, **41**, 3489; M. Schwickardi, T. Johann, W. Schmidt and F. Schüth, *Chem. Mater.*, 2002, **14**, 3913; Y. D. Xia and R. Mokaya, *J. Mater. Chem.*, 2005, **15**, 3126.
10 W. Li, A.-H. Lu and F. Schüth, *Chem. Mater.*, 2005, **17**, 3620.
11 W. Li, A.-H. Lu, C. Weidenthaler and F. Schüth, *Chem. Mater.*, 2004, **16**, 5676.
12 W. Li, A.-H. Lu, W. Schmidt and F. Schüth, *Chem.–Eur. J.*, 2005, **11**, 1658.
13 W. Li, A.-H. Lu, R. Palkovits, W. Schmidt, B. Spliethoff and F. Schüth, *J. Am. Chem. Soc.*, 2005, **127**, 12595.
14 M. Haruta, S. Tsubota, T. Kobayashi, H. Kageyama, M. J. Genet and B. Delmon, *J. Catal.*, 1993, **144**, 175.
15 C. K. Costello, M. C. Kung, H.-S. Oh, Y. Wang and H. H. Kung, *Appl. Catal., A*, 2002, **232**, 159.
16 J. Guzman and B. C. Gates, *J. Am. Chem. Soc.*, 2004, **126**, 2672.
17 J. C. Fierro-Gonzalez, V. A. Bhirud and B. C. Gates, *Chem. Commun.*, 2005, 5275.
18 M. Comotti, W. Li, B. Spliethoff and F. Schüth, *J. Am. Chem. Soc.*, 2006, **128**, 917.
19 J.-D. Grunwaldt and H. Teunissen, *US Patent*, 6 692 713 B2, 2004.